



Operability robustness index as seakeeping performance criterion for offshore vessels

Martin Gutsch^{a,b,*}, Sverre Steen^a, Florian Sprenger^c

^a Norwegian University of Science and Technology, Trondheim, Norway

^b SINTEF Ocean, Trondheim, Norway

^c Forschungszentrum Jülich, Berlin, Germany

ARTICLE INFO

Keywords:

Offshore vessel

Seakeeping performance

KPI

Design parameter

Operability robustness index

Percentage operability

ABSTRACT

The offshore industry operates increasingly large installations in exposed areas requiring high reliability and availability. Downtime of complex offshore systems leads to significant financial losses. Towards year-round offshore installation and maintenance service, this research focuses on the identification of weather-robust vessel designs. Even though it might seem that the motions of a larger vessel will be more favorable than those of a smaller vessel, this research shows that this hypothesis is not necessarily true. It will be shown that for certain vessel parameters the performance of a larger vessel is not better than that of a smaller vessel. This investigation aims to provide knowledge for a more holistic vessel design optimization approach to enable ship designers and operators to design and select an offshore vessel with main dimensions and hydrostatic parameters providing optimal seakeeping performance for a given operation and environment. The key aspect is a mission-dependent optimization of hull dimensions, including loading condition parameters, aiming for a hull design where natural periods of important responses such as pitch and roll are significantly distinct from the dominating wave periods. For this purpose, a novel parameter for seakeeping performance evaluation, the Operability Robustness Index (ORI), will be used.

1. Introduction

The optimization of seakeeping performance is the improvement of the vessel's capability to efficiently execute its mission despite adverse weather conditions (Comstock and Keane, 1980). The investigation of the dependency of vessel dimensions and loading conditions on the behavioral vessel response in waves is crucial for the determination of operational performance as well as the design and selection of the best-suited vessel. Strategies for identification and benchmarking of operational performance, based on non-exceedance of specified motion limitations, remain a significant area of interest for hull optimization. A practical approach for the assessment of vessel motion performance in waves will support ship designers and operators to design and select the best suited vessel for defined operational scenarios. The proposed methodology is applicable for a wide range of offshore vessels, such as offshore construction vessel (OCV), inspection maintenance and repair vessel (IMR), anchor handling vessel (AHV), platform supply vessel (PSV), as well as accommodation vessel, and crew transfer vessel.

A tendency towards increasingly rough weather conditions triggered by climate change (Young and Ribal, 2019), combined with a growing financial pressure, within the complete offshore value chain (Mellbye

et al., 2017) leads to the need of a more thorough evaluation and optimization of mission oriented seakeeping performance.

During the last decade, designers, operators, and clients, working in the oil and gas business, indicated a demand for larger OCVs, mainly to ensure high operational performance by minimizing the risk for delays due to possible weather related waiting time. The fact that vessel size is not necessarily decisive for the assessment of seakeeping performance is known in literature (Papanikolaou, 2014), however, it is commonly misinterpreted within the offshore construction industry. Therefore, the presented research shall contribute to the identification of potential for performance improvement aiming for increased mission performance and/or a reduction in vessel size and thus operational costs. Although ship design is always a balance of various functions, this is a feasible approach at an early design stage, since an increased OCV hull size is often motivated by seakeeping optimization purpose and not loading requirements as it is usually the case for other ship types.

The quest for an optimal vessel design minimizing the adverse impact and degradation of ship performance caused by the sea environment, has been an intense area of research for decades. In commercial navigation, vertical accelerations and relative motions between hull

* Corresponding author.

E-mail address: martin.gutsch@sintef.no (M. Gutsch).

and wave are identified as critical for favorable seakeeping performance (Faltinsen, 1990). It is therefore reasonable that the minimization of heave, pitch, and vertical ship motions, as well as accelerations, exclusively at forward speed, have been the main research objectives. Lewis (1955) investigated the influence of a forebody design on seakeeping performance in extreme weather conditions. This paper experimentally compared the u-shaped Series 60 hull model with another model having the same main dimensions and buoyancy distribution, but with extreme v-shaped sections in the forebody. Swaan and Vossers (1961) and Swaan (1961) extended these tests in regular bow waves (10° and 50° off head seas) comparing seakeeping performance of the original u-shaped Series 60 hull with three other models with differently v-shaped bow sections and at two forward speeds. Bengtsson (1962) extended the test series with seven models for a larger range of forward speeds in regular head seas. In 1965, he extended his series by further investigations of the influence of block coefficient and ballast draught condition on seakeeping performance (Bengtsson, 1965).

Bales and Cummins (1970) performed parametric seakeeping calculations in a relatively large study, using seven parametrically altered design parameters adopted on a simplified hull design. Ewing (1967) performed numerical seakeeping analysis on the Series 60 model which was continued and extended by Yourkov (1973) and Beukelman and Huijser (1976). The progress in numerical calculations allowed Loukakis (1975) to investigate seakeeping performance in head waves for seventy two hull forms for the extended Series 60 design. Loukakis findings for heave, pitch, bending moment, and added resistance are presented as seakeeping tables, allowing the linear interpolation of the results as function of principle hull characteristics, Froude number, and sea state. As a result of the presented studies it can be concluded that the ship length appeared to have a greater influence on seakeeping performance, while the forebody section shape and the block coefficient showed a smaller influence on seakeeping performance (Beukelman and Huijser, 1976). Generally, local hull modifications show a minor impact on motion performance, whereas the increase in hull length results in a noticeable increase in performance (Lloyd, 1989). Accordingly, larger ships tend to be more comfortable than smaller ships and the increase in hull size will result in improved seakeeping performance. “Seakeeping performance assessment must therefore be considered at an early stage in the design process before the major proportions and dimensions of the hull have been settled” (Lloyd, 1989). In more recent years, the research focus has been rather on the optimization procedures of particular vessel designs than on the exploration of the designs parameters influence on seakeeping performance, being the primary objective of the current study.

The influence of design parameters on ship motions has been a research topic in the past decades and is relatively well understood. Nonetheless, Norwegian offshore vessel designers are indicating strong interest in further investigations of the impact of vessel design characteristics on seakeeping performance. In the context of offshore lifting operations, roll and pitch are generally most critical motion components. While vertical motion components can be compensated by the crane’s automated heave compensation system, horizontal crane tip motions, as a result mainly from roll, cannot be compensated and limit operability, especially during the lift-in-air phase.

The focus of this work is on the systematic presentation of the influence of design parameters on roll at zero ship speed to identify and benchmark mission-oriented seakeeping performance. For this purpose, the percentage operability and the Operational Robustness Index (ORI), introduced by Gutsch et al. (2016, 2017), will be utilized. Both performance parameters are suitable for the identification and benchmarking of mission-oriented vessel capabilities related to a selected motion parameter, sea area, and season. A comparison between the two parameters will be presented and the differences in application and analysis will be discussed based on selected results from a large

database of motion transfer functions of parametrically re-sized geometric similar vessel designs. The basic hull geometry is provided by a ship designer, representing a typical modern offshore construction vessel in operation since 2014. The origin of this design is agreed to be confidential. However, the complete RAO database can be used for further investigation and is accessible online by using the Vessel Response Tool, freely accessible on vrt.sintef.no.

2. Assessment of operational performance

Marine operations, especially walk-to-work (W2W) and lifting operations over the vessel’s hull side require a specialized vessel designs with high operability. DNV GL’s offshore standard for marine operations states: “A marine operation shall be designed to bring an object from one defined safe condition to another” (DNV GL, 2011). The term *safe condition* refers to a condition in which the object is exposed to the same level of risk for damage or loss as in the in-place condition. However, between those safe conditions, the object will be exposed to movements and water impact forces which must not exceed a maximum tolerable level, defined in terms of motion limitation criteria such as: motion displacements, velocities, or accelerations. Information on motion limitations, or non-exceedance criteria are used for vessel operability analysis together with weather hindcast data, leading to a determination of the vessel’s operability, often also referred to as seakeeping theperformance.

Vessel operability is defined as the ability to carry out the vessel’s mission safely while the environmental impact, represented by the waves, degrades this operability compared to the calm water condition. In order to optimize operability, vessel motions must be minimized. Lower vessel motion levels will be achieved by moving natural periods of vessel motions outside the range of typical wave periods, encountered in the sea area of interest, and by increasing the damping effectiveness. An example of an effective damping device to reduce roll motions are bilge keels.

The overall purpose of seakeeping optimization is to reduce the vessel’s sensitivity to environmental conditions, therefore, increasing operability, availability, and safety towards year-round offshore operations.

To evaluate of vessel operability, a study of wave induced vessel response characteristics is essential. As an example, lifting operability will be optimized by minimizing crane tip motions. Generally, it can be differentiated between vessel motions excited by first- and second order wave forces. While second order forces, leading to drift motions can be substantially minimized by a well-tuned dynamic positioning (DP) system, motions, excited by first order wave forces cannot be completely suppressed. Horizontal and vertical motions in the wave period frequency range are mainly caused by the vessel’s heave, roll, and pitch motions, and can be minimized by well-chosen design parameters which will be further addressed.

Although roll motions can be efficiently reduced by damping devices such as bilge keels and roll reduction tanks (RRTs), which on one hand are a well-proven strategy to reduce unwanted roll motions for W2W operations, on the other hand, however, free surface RRTs reduce vessel stability. Due to the effect of the free surface, the use of those highly efficient roll damping devices might be a risk during the execution of marine operations, directly affecting the vessel’s stability, such as offshore lifting- or anchor handling operations. The stability reduction due to a RRT has most likely been one of the leading reasons to the capsizing accident of the AHV Bourbon Dolphin, analyzed by Lyng et al. (2008). Furthermore, response optimization can be achieved to some degree by particular hull shapes with a reduced water line area, such as specialized multihull designs, examples being Small Waterplane Area Twin Hull (SWATH) and Semi-submersible designs. Yet, those specialized vessels are rather rare exceptions among offshore vessels and will not be further discussed.

Table 1
Phases of a subsea lifting operation.

| | Hazards | Vessel response cause |
|--|---|--|
| Lift-off: | Tension in lifting wire. Horizontal motion of object after lift-off due to misalignment of object and crane tip. | No direct vessel response dependent cause for hazards are identified. |
| Object in air: | Uncontrolled horizontal motions. Collision with ship structure (e.g. hull, crane superstructure) and personnel. Crane capacity decrease over crane radius. Limited lifting height. | Horizontal crane tip motions due to roll and pitch motions. Match of horizontal pendulum period with period of horizontal vessel motions. |
| Splash zone: (passing the water surface) | Overload due to strongly varying dynamic forces. Slack in lifting line followed by snatch peak loads due to slamming, added mass, and other hydrodynamic forces. | Vertical crane tip velocity (mainly due to roll and heave motions) relative to wave elevation. Vertical crane tip acceleration. |
| Lowering through water column: | Crane peak loads and excitation of parametric rolling due to increased lifting line length and/or activated heave compensation system. Increasing load component of steel wire in deeper waters. | Match of natural roll period with natural period of the crane, due to the elasticity of the crane structure and the wire which is variable over line length. |
| Landing on seabed: (including position adjustments) | Vertical motions of object. Insufficient accuracy of horizontal positioning. Poor underwater visibility at landing zone. Crane overload due to the additional wire weight force of the longer lifting line in extra deep waters. | Accuracy of dynamic positioning (DP) capability. Absolute vertical crane tip velocity due to roll motions. |

2.1. Phases of a lifting operation

A subsea crane operation over the vessel's hull side can be divided into five operational phases summarized in Table 1. Each phase is associated with specific hazards, which have to be identified during the planning process and evaluated during vessel design and selection to be kept within acceptable limits. Generally, horizontal crane tip displacements and periods are more critical during lift-off and object in air lift, while relative vertical velocities and accelerations may be critical in the splash zone. The lift through the water column may become critical, especially for deep water operations. Due to the elasticity and the weight of the lifting line, the longer crane wire will affect the natural vertical period of the crane system. The accordance of this natural period with, for example the roll period, must be avoided. Finally, an accurate DP system and a limited absolute vertical velocity at crane tip position is required to allow the object to be safely positioned and landed on the seabed.

2.2. Seakeeping analysis

A seakeeping analysis is based on the detailed knowledge of the planned operational task. Mission requirements, as illustrated in Fig. 1, define the starting point of an operability analysis. For the design or the selection of a suitable vessel, information on the required payload, the ship speed, the motion limitation(s), the preferred wave heading, and the expected weather must be available. The required payload determines the vessel's mass distribution and will affect its hydrostatic properties and thus its response characteristics in waves. The combination of the wave spectrum, expected at the sea area and season of interest, with the general vessel response characteristics leads to the actual vessel behavioral response. A comparison with mission dependent motion limitations, including possible limitations based on sensitive on-board equipment leads to the overall vessel seakeeping performance. Besides technical aspects contributing to seakeeping performance, the evaluation of human factors (including crew competence, organization, and safety components) will complete the analysis.

The individual calculation steps towards a seakeeping performance value such as the Percentage Operability (percOP) or the Operational

Robustness Index (ORI) are shown in Fig. 2. By using the hydrodynamic characteristics of the hull, including mass distribution, wave heading, and ship speed, the transfer function of the hull motions, characterized by the Response Amplitude Operator (RAO) and phase angle, can be determined. For the current study, the RAOs are calculated with SINTEF Ocean's VESSEL RESPONSE calculation software VERES, based on linear strip theory (Salvesen et al., 1970; Fathi, 2017).

Assuming linear behavior, the harmonic excitation of the vessel due to a wave of the frequency ω yields a phase shifted harmonic response of the same frequency. The RAO describes the ratio between the response output signal $s_j(\omega)$ and the wave excitation input signal $\zeta(\omega)$, for each six degrees of freedom (6DOF) motion mode j , circular wave frequency ω , and heading β . This motion transfer function provides a full correlation of the hydrodynamic motion characteristics for a defined heading β and ship speed in regular waves:

$$H_j(\omega; \beta) = \frac{s_j(\omega; \beta)}{\zeta(\omega)} \quad (1)$$

The RAOs, determined within the current study, accounted for viscous roll damping due to frictional shear stress on the hull surface (Kato, 1957), eddy damping (Ikeda et al., 1977a), and lift damping from pressure variation along the naked hull (Himeno, 1981), damping contributions from bilge keels due to normal forces (Ikeda et al., 1976), and hull pressure created by the presence of the bilge keels (Ikeda et al., 1977b). The damping contribution of a typical bilge keel size, being a third of the hull length ($L_{hull}/3$) by 30 cm width, is assumed. At zero speed, wave radiation damping is obtained from analysis of each single strip. Contributions of non-linear damping effects are included, using a significant wave height of 2 m to linearize the non-linear roll damping component.

According to the recommendation by DNV GL for the North Sea and North Atlantic, the JONSWAP (Joint North Sea Wave Project) wave spectrum with a variable peakedness parameter γ describing both, steep wind-driven and longer swell dominated waves is used DNV GL (2017, section 3.5.5.5).

Once the suitable sea state spectra $S_\zeta(\omega; T_p)$ with the associated range of peak periods are established, the stochastic analysis begins with the determination of the desired response spectra $S_j(\omega; \beta; T_p)$ by

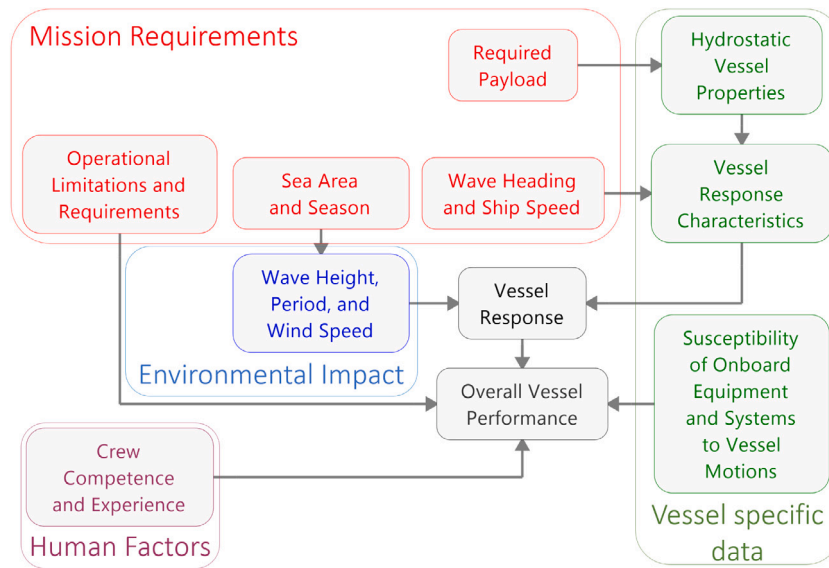


Fig. 1. Schematic representation of information flow for operability analysis.

multiplying the sea state spectra by the squared absolute value of the RAO for each mode j :

$$S_j(\omega; \beta; T_p) = |H_j(\omega; \beta)|^2 S_\zeta(\omega; T_p) \quad (2)$$

From the area enclosed by the response spectra, standard deviation $\sigma_j(\beta; T_p)$ and significant double amplitudes $\eta_{j_s}(\beta; T_p)$ for the individual heading β are determined:

$$\sigma_j(\beta; T_p) = \sqrt{\int_0^\infty S_j(\omega; \beta; T_p) d\omega} \quad (3)$$

$$\eta_{j_s}(\beta; T_p) = 4 \sigma_j(\beta; T_p) \quad (4)$$

Finally, the maximum tolerable significant wave height $H_{s,tol}(\beta; T_p)$ can be calculated by multiplying the maximum tolerable motion criteria $\sigma_{j,tol}$ with the ratio of the significant wave height and the values obtained from Eq. (3):

$$H_{s,tol}(\beta; T_p) = \sigma_{j,tol} \frac{H_s}{\sigma_j(\beta; T_p)} \quad (5)$$

By comparison of the maximal tolerable wave height $H_{s,tol}(\beta; T_p)$ for the individual heading β with the wave scatter diagram from a defined sea area and season, the percentage operability $P_{OP}(\beta)$ can be determined for the selected heading. Generally, percentage operability expresses the percentage of the time where the vessel can satisfy the maximum tolerable operability limitation criteria $OP_{tol,max}$ for a given sea state, described by H_s and T_p .

The minimization of roll motions is a major objective during offshore vessel design. For the vessel design, as well as in the scenario of a vessel selection process during operational planning, the selection of a correct quantitative motion limitation value is less important than the general capability of the vessel to show high operability, even for low, and thus strict motion limitations. To satisfy this characteristic, the operability analysis will be performed for several motion limitations between zero and a maximum limit. This allows to create a curve showing percentage operability performance P_{OP} evolving between zero and the specified maximum tolerable operational limit $OP_{tol,max}$ as indicated by the large graph on Fig. 3. Based on the initial steepness of the curve, the vessel with the highest operability for strict motion limitations can be identified. Generally, the steeper the curve, showing a higher gradient, the better the global performance. For this analysis, the maximum tolerable operational limit can be chosen rather freely, but must be kept constant throughout the complete benchmarking

process. For the analysis of roll performance this can be a maximum tolerable root mean square (RMS) value for roll of 1° or even 2° . Fig. 3 shows an example that the roll limitation criterion of 2.0° RMS leads to an absolute percentage operability (percOP) of about 100% for all variations of GM_T during North Sea summer season, while the initial steepness of the compared loading condition indicates different motion sensitivity levels on smaller waves.

The new Operability Robustness Index (ORI) is introduced as Eq. (6) to express the global performance of a ship for a selected motion criterion. The ORI is expressed as a single benchmark parameter by the dimensionless ratio of the area enclosed by the curves on the large graph in Fig. 3, exemplarily indicated by the gray area below the red curve, and the maximum theoretically possible operability which is be equivalent to the product of $OP_{tol,max}$ and 100% operability, indicated by the black dashed rectangular line. The small graph on Fig. 3 represents the development of the ORI over the motion limitation extracted from the large percentage operability (percOP) graph.

$$ORI = \frac{\int_0^{OP_{tol,max}} P_{OP}(OP_{tol}) d(OP_{tol})}{OP_{tol,max} \cdot 100} \quad (6)$$

For the quantification of response-based operability this new performance parameter was first introduced by Gutsch et al. (2016), and is used by Gutsch et al. (2017) and Sandvik et al. (2018).

In comparison to the absolute percOP value, the use of the ORI has clear advantages for benchmarking of the relative response performance of different vessel designs. Since the ORI includes the evaluation of the percOP for a specified range of operational limits, including low and hence strict values, the result of the performance assessment is less dependent on the choice of the maximum allowable limitation value. For this reason, the ORI provides a broader view on response-based vessel performance. Therefore, complementary to the percOP, the ORI is perceived as a *quality index* for vessel performance in waves with respect to a selected motion criterion and is therefore perfectly suitable as Key Performance Indicator (KPI) for seakeeping performance.

3. Parametric design variation

A parametric investigation utilizing the geometry of a modern offshore construction vessel (OCV) design is conducted. The applied geometry is scaled to five different hull lengths (L_{hull}) between 80 m and 160 m. For these parent hull geometries of five different hull length (L_{hull}), the beam (B_0) is adapted to represent a realistic average length-to-beam ratio (L_{hull}/B_0) as found to be typical for OCVs of each

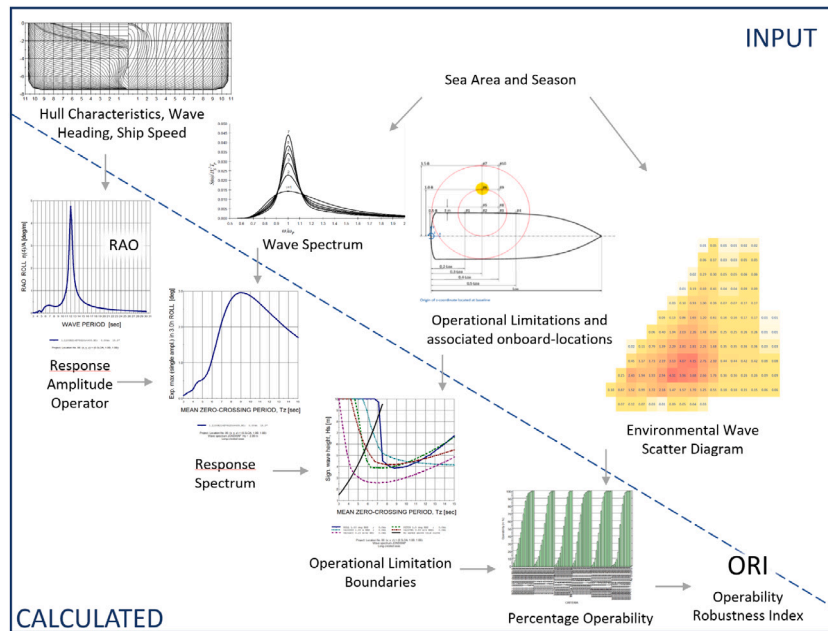


Fig. 2. Individual calculation steps for operability analysis.

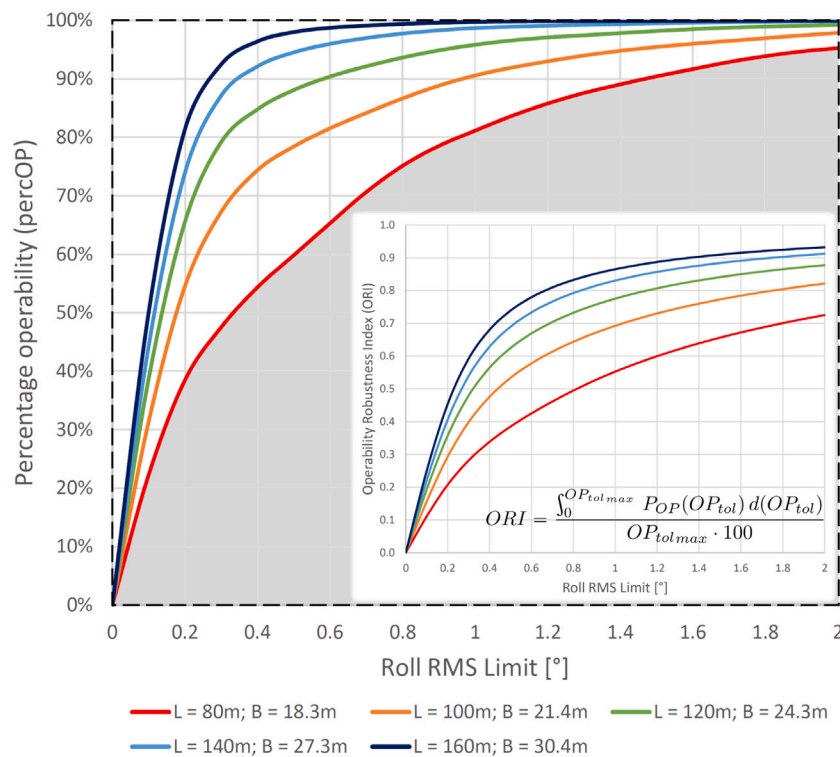


Fig. 3. Derivation of the Operability Robustness Index from percentage operability. For coloured representations consult the open access web version.

corresponding length. For this reason the length dependent L/B ratio of fifty currently operating OCVs of hull lengths between 67 m and 180 m is analyzed. The following polynomial formulation is found:

$$B_0 = \frac{1}{-6.762 \cdot 10^{-5} \cdot L_{hull} + 2.730 \cdot 10^{-2} + \frac{2.627}{L_{hull}}} \quad (7)$$

The hydrodynamic characteristics of the initial vessel designs with average length-to-beam ratio (L_{hull}/B_0) are indicated in Table 2.

Based on the initial vessel designs with five hull lengths and the typical beams (B_0), derived from Eq. (7) as indicated in Table 2, the

actual beam (B) is increased and reduced in steps of one meter, to a range of plus/minus three meters, resulting in a set of 35 different hull sizes as shown in Table 3. For each of the 35 hull designs, the roll response amplitude is analyzed for nine draughts (D) between 5 m and 9 m and nine transverse metacentric heights (GM_T) between 1 m and 5 m (see Fig. 4) resulting in a database of 2835 Response Amplitude Operators (RAOs) for geometrically similar vessel designs. Since the height of the metacenter is defined by the cross-sectional geometry of the vessel, the vertical center of gravity (VCG) is adjusted in order to achieve the desired GM_T value. The distribution of mass in transverse

| | | Hull length L_{hull} [m] | | | | | | | | | | |
|----------|-------|----------------------------|--------------------------------|-------|-------|-------|-----|-----|-----|-----|-----|-----|
| | | 80 | 100 | 120 | 140 | 160 | | | | | | |
| Beam [m] | -3.0 | 15.30 | 18.40 | 21.30 | 24.30 | 27.40 | | | | | | |
| | -2.0 | 16.30 | Metacentric height, GM_t [m] | | | | | | | | | |
| | -1.0 | 17.30 | Draught [m] | 1.0 | 1.5 | 2.0 | 2.5 | 3.0 | 3.5 | 4.0 | 4.5 | 5.0 |
| | B_0 | 18.30 | 5.0 | x | x | x | x | x | x | x | x | x |
| | | | 5.5 | x | x | x | x | x | x | x | x | x |
| | | | 6.0 | x | x | x | x | x | x | x | x | x |
| | +1.0 | 19.30 | 6.5 | x | x | x | x | x | x | x | x | x |
| | +2.0 | 20.30 | 7.0 | x | x | x | x | x | x | x | x | x |
| | | | 7.5 | x | x | x | x | x | x | x | x | x |
| | +3.0 | 21.30 | 8.0 | x | x | x | x | x | x | x | x | x |
| | | 8.5 | x | x | x | x | x | x | x | x | x | |
| | | 9.0 | x | x | x | x | x | x | x | x | x | |

Fig. 4. Variation of design parameters draught (D) and metacentric height (GM_T).

Table 2
Hydrodynamic characteristics of parent hull designs.

| Hull length | L_{hull} | [m] | 80 | 100 | 120 | 140 | 160 |
|--------------------------------|------------|-----|-------|--------|--------|--------|--------|
| Length between perpendiculars | L_{pp} | [m] | 72.48 | 90.60 | 108.72 | 126.84 | 144.97 |
| Beam | B_0 | [m] | 18.30 | 21.40 | 24.30 | 27.30 | 30.40 |
| Draught | D_0 | [m] | 7.5 | 7.5 | 7.5 | 7.5 | 7.5 |
| Metacentric height | GM_{T0} | [m] | 2.5 | 2.5 | 2.5 | 2.5 | 2.5 |
| Displacement | Δ | [t] | 7 699 | 11 253 | 15 334 | 20 833 | 25 575 |
| Block coefficient | C_B | [-] | 0.755 | 0.755 | 0.755 | 0.755 | 0.755 |
| Vertical center of gravity | VCG | [m] | 5.89 | 7.46 | 9.15 | 11.83 | 13.41 |
| Longitudinal center of gravity | LCG | [m] | 35.87 | 44.84 | 53.81 | 62.78 | 71.75 |
| Radius of gyration for roll | R_{44} | [m] | 6.405 | 7.49 | 8.51 | 9.91 | 10.64 |
| Radius of gyration for pitch | R_{55} | [m] | 18.12 | 22.65 | 27.18 | 31.71 | 36.24 |
| Radius of gyration for yaw | R_{66} | [m] | 18.12 | 22.65 | 27.18 | 31.71 | 36.24 |

Table 3
Investigated (beam) values for the variation of beam.

| | Hull length L_{hull} [m] | | | | | |
|----------|----------------------------|-------|-------|-------|-------|-------|
| | 80 | 100 | 120 | 140 | 160 | |
| -3.0 | 15.30 | 18.40 | 21.30 | 24.30 | 27.40 | |
| -2.0 | 16.30 | 19.40 | 22.30 | 25.30 | 28.40 | |
| -1.0 | 17.30 | 20.40 | 23.30 | 26.30 | 29.40 | |
| Beam [m] | B_0 | 18.30 | 21.40 | 24.30 | 27.30 | 30.40 |
| | | 19.30 | 22.40 | 25.30 | 28.30 | 31.40 |
| | | 20.30 | 23.40 | 26.30 | 29.30 | 32.40 |
| | | 21.30 | 24.40 | 27.30 | 30.30 | 33.40 |

(mass moment of inertia for roll $R_{44} = 0.35 \cdot beam$) and longitudinal (mass moment of inertia for pitch $R_{55} = 0.25 \cdot L_{pp}$, length between perpendiculars) direction is kept constant for all vessel designs. All parameters are treated as isolated variables by taking into account their relation and dependency on other vessel parameters, which are adapted as shown in Table 4. The ranges of the parameter variations, from lowest to highest, intentionally exceed their typical ranges for OCVs, especially for GM_T .

The isolated variation of single parameters, irrespective of its subsequent physical relationship to other parameters, might be an academic approach with vessel particulars which are not always applicable in a real vessel design. However, it provides the researcher with a method to identify important parameters that influence operability. The dependencies of the altered parameters on other vessel characteristics are shown in Table 4. A variation of the mass moment of inertia for roll (R_{44}) and pitch (R_{55}) is not carried out, since the controllability of this value is usually very limited in practical operation. Nevertheless, results from a small parametric study for R_{44} are published by Gutsch et al. (2016, 2017).

Table 4
Dependencies of varied parameters.

| Varied parameter | Constant values ^a | Adapted values ^a |
|-------------------------------|--|-------------------------------|
| Hull length (L_{hull}) | $D_0; GM_{T0}; VCG; \frac{R_{44}}{B_0}$ | $R_{55}; B_0; R_{44}; \nabla$ |
| Beam (B) | $D_0; GM_{T0}; L_{hull}; \frac{R_{44}}{B}; R_{55}$ | $VCG; R_{44}; \nabla$ |
| Draught (D) | $B_0; GM_{T0}; L_{hull}; R_{44}; R_{55}$ | $VCG; \nabla$ |
| Metacentric height (GM_T) | $B_0; D_0; L_{hull}; R_{44}; R_{55}; \nabla$ | VCG |

^aNote: Vertical center of gravity (VCG), mass moment of inertia for roll (R_{44}), mass moment of inertia for pitch (R_{55}), displacement (∇); the index 0 refers to the values selected for the parent hull designs as shown in Table 2.

4. Analysis of roll amplitude

The seakeeping performance of geometric similar offshore vessel designs is analyzed to investigate the influence of the variation of hull length (L), beam (B), draught (D), and transverse metacentric height (GM_T) in the North Sea (56.52N, 3.24E) and North Atlantic (65.29N, 7.32E), both, during the winter and summer seasons. As environmental information, metocean hindcast data, obtained between 1958 and 2016, provided by the Norwegian Meteorological Institute, is used. The performance is benchmarked in terms of percentage operability (percOP) and the Operational Robustness Index (ORI).

All results presented in this chapter are calculated based on vessel motion characteristics at zero speed. Further, a wave heading of 30°, corresponding to bow-quartering seas,¹ and a limiting roll angle of 0.5°, 1.0°, and 2.0° root-mean-square (RMS) are exemplarily chosen for

¹ In VERES a wave heading angle of 0° corresponds to head seas, 90° corresponds to beam seas, and 180° corresponds to following seas.

the analysis. In practical day to day work, the limitations should be evaluated individually according to the requirements of the specific offshore operation. The wave heading of 30° off-bow represents a typical situation during an offshore lifting task or a W2W operation. The choice of this wave angle is considered; although, a wave angle of 15°, corresponding to almost head seas, could be preferred in practical operations to minimize roll and still provide favorable wave shielding effects for e.g. the splash zone area. However, to simplify the calculations a long-crested wave spectrum is chosen for the analysis. Therefore, the slightly larger wave angle of 30° shall provide slightly more roll response and account for a potentially more scattered wave energy spreading in real sea conditions. The choice of the long-crested sea spectrum is based on practical reasons; due to the comparative nature of the study, main focus is placed on the comparison of relative results between the different designs. With the objective to provide understanding of influencing factors allowing a better identification of favorable vessel design parameters. For this purpose, the long-crested sea spectrum is regarded as more appropriate than a short-crested directional wave spectrum which would rather allow the best possible modeling of real sea conditions but also involves further influencing factors which must be taken into consideration in the analysis of the results.

In order to limit the amount of results, a reduced set of results with the most relevant variations is selected. The interested reader is invited to perform further analysis using the online Vessel Response Tool, freely available on vrt.sintef.no.

4.1. Presentation of results

The results for the variation of length (Fig. 5), beam (Figs. 7 and 8), draught (Figs. 10 and 11), and GM_T (Figs. 13 and 14) are illustrated by the percOP (red graph², related to primary ordinate) and the ORI (blue graph², related to secondary ordinate). For both performance benchmarks the same roll angle limitation criteria are used, for each limitation criterion a set of five curves that show the results of the different hull lengths over the related parameter as indicated below the abscissa. The related hull lengths are indicated for the variation of beam by arrows (Figs. 7 and 8), whereas for the variation of draught and GM_T each hull length is presented separately in a sub-diagram (Figs. 7, 8, 10, 11, 13, and 14).

Additionally, the results are visualized as color maps², indicating the numerical variation of the investigated parameters for the 2° RMS roll angle limitation criterion. These color maps are shown for the variation of length in Fig. 6, for beam in Fig. 9, for draught in Fig. 12, and for GM_T in Fig. 15. As in the diagrams, the color maps show the results obtained during winter season, in North Sea and North Atlantic, in a table-like presentation for each altered vessel parameter per rows. While in columns, on the left side the absolute value for the percOP and the ORI are shown, followed by the mean value and the spreading of the results for each vessel length. Finally, on the right side the deviation (that means the relative difference) of the mean value is presented. The definition of the color code is indicated in the legend below and can be summarized as followed (from left to right side):

- The color code² behind the absolute value indicates the level of the result above 75% for percOP and 0.5 for ORI in green and below that value in red. A fully developed green color indicates a value approaching 100% (for percOP), or 1.0 (for ORI), respectively. A fully developed red color indicates a value of 50% or lower for percOP and approaching 0.0 for ORI. The color scale is selected individually to best represent the deviating levels of the result.

- The color bar behind the mean value and the spread shows the percOP in red (for its range between 0% and 100%) and the ORI in blue (for its range between 0 and 1).
- The color code behind the deviation to the mean value indicates the level of an increase above 0% for percOP and 0.0 for ORI in green and decrease below that value in red. A fully developed green color indicates a deviation to the mean of $\geq 25\%$ for percOP and ≥ 0.2 for ORI. A fully developed red color indicates a deviation to the mean of $\leq 25\%$ for percOP and ≤ 0.2 for ORI. Again, the color scale is selected individually to better present the deviating levels of the result.

The individual levels for the color codes are selected according to the general range of the presented results and since an increase or decrease of 20% to 25% indicate a significant performance gain or loss compared to an average value and will considerably influence vessel performance.

4.2. Winter season versus summer season

The analysis of the vessel performance during winter versus summer season shows a significant increase in roll performance (expressed in terms of percOP and ORI) during the summer season (Figs. 5, 7, 8, 10, 11, 13, and 14). The absolute difference between the highest and lowest performance, is nominated as spread in Fig. 6, it is larger for the season and area with the roughest weather condition, (which generally is North Atlantic and winter season) while it is significantly smaller during summer season, when the performance characteristics are generally adequate for all vessels. This is especially observed in the analysis of the percOP, while the ORI is still capable of indicating the differences between the designs, the percOP value converges against 100% and is not capable of indicating performance variations. This is related to the fact that the percOP indicates the absolute performance for the chosen limitation criterion. Therefore, the percOP value approaches a value close to 100% during the summer season almost regardless of the vessel's capabilities during the winter season. This is the case for the percOP value when calculated for a fairly calm environmental condition (such as encountered during summer season) and/or for a rather large motion limitation (such as the 2° RMS roll value or higher). Therefore, if the result for the percOP approaches 100%, representing the maximum achievable value for percOP, a proper performance assessment and benchmarking of the deviating vessel designs becomes impossible. In comparison to the percOP, the ORI accounts for the development of the percOP on its complete course of this behavior between zero and the chosen maximum motion limitation. Therefore, the ORI behaves qualitatively similar but approaching its maximum possible value of 1.0 slower. Consequently, the ORI allows vessel performance assessment to be more independent of the chosen environmental condition and level of limitation criteria.

Aiming for year-round offshore operations, a design optimization focusing on the improvement of operability during the winter season is required. Therefore, this research will mostly focus on the analysis of design dependent results for percOP and ORI during the winter season.

4.3. North Sea versus North Atlantic

As a general remark it can be stated that roll performance results (expressed in terms of percOP and ORI) are higher in North Sea than in the North Atlantic independently of the investigated vessel design.

The comparison between North Sea versus North Atlantic winter season, indicates that the North Sea has a larger increase in roll performance for shorter vessels between 80 m and 100 m hull length, while this increase is reduced for longer vessels between 140 m and 160 m (Fig. 5). The results analyzed for the North Atlantic however, show with a larger operability gain for longer hull lengths, being the opposite behavior. This may be an indication that in a more holistic

² For the representation of the results in coloured figures please refer to the open access web version of this article.

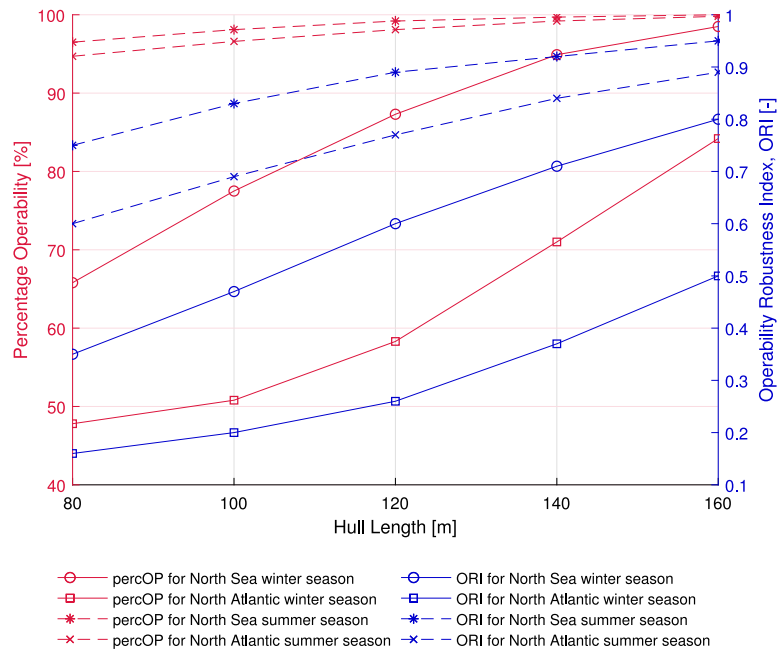


Fig. 5. Operability as function of hull length for 2° roll angle RMS criterion. For coloured representations consult the open access web version.

| | Absolute value for length variation | | | | | Deviation from mean for length variation | | | | | | |
|------------------------|-------------------------------------|-----------|-----------|-----------|-----------|--|--------|-----------|-----------|-----------|-----------|-----------|
| | L = 80m | L = 100m | L = 120m | L = 140m | L = 160m | Mean | Spread | B = 18.3m | B = 21.4m | B = 24.3m | B = 27.3m | B = 30.4m |
| | B = 18.3m | B = 21.4m | B = 24.3m | B = 27.3m | B = 30.4m | | | | | | | |
| percOP [%] | 65.8 | 77.5 | 87.3 | 94.9 | 98.5 | 84.8 | 32.6 | -19.0 | -7.3 | 2.5 | 10.1 | 13.7 |
| North Sea, winter | 47.8 | 50.8 | 58.3 | 71.0 | 84.2 | 62.4 | 36.4 | -14.6 | -11.6 | -4.1 | 8.6 | 21.8 |
| North Atlantic, winter | 95.3 | 97.9 | 99.2 | 99.9 | 100.0 | 98.4 | 4.7 | -3.2 | -0.6 | 0.8 | 1.4 | 1.5 |
| North Sea, summer | 93.0 | 96.0 | 98.0 | 99.4 | 99.9 | 97.2 | 6.9 | -4.3 | -1.3 | 0.8 | 2.1 | 2.6 |
| North Atlantic, summer | 0.35 | 0.47 | 0.60 | 0.71 | 0.80 | 0.39 | 0.46 | -0.24 | -0.11 | 0.01 | 0.13 | 0.22 |
| ORI [-] | 0.16 | 0.20 | 0.26 | 0.37 | 0.50 | 0.30 | 0.34 | -0.14 | -0.10 | -0.04 | 0.07 | 0.20 |
| North Sea, winter | 0.73 | 0.83 | 0.89 | 0.93 | 0.95 | 0.86 | 0.22 | -0.13 | -0.04 | 0.02 | 0.06 | 0.08 |
| North Atlantic, winter | 0.56 | 0.67 | 0.76 | 0.84 | 0.90 | 0.75 | 0.33 | -0.18 | -0.08 | 0.02 | 0.10 | 0.15 |
| North Sea, summer | | | | | | | | | | | | |
| North Atlantic, summer | | | | | | | | | | | | |

Fig. 6. Absolute and relative results for length variation and 2° roll angle RMS criterion. For coloured representations consult the open access web version.

cost/benefit evaluation process an optimal seakeeping performance may be identified for hull lengths, which are in most cases generally shorter in the North Sea than in the North Atlantic. However, a more detailed analysis of the influence of specific design variations indicates deviating behavior due to the different dominating wave peak period T_p as discussed in Section 4.7.

4.4. Variation of length

For most of the results, roll performance is improving with larger hull lengths (L_{hull}) and vessel displacements (V) as shown in Fig. 5). This tendency is expected, since for each length a common length-to-beam ratio (L_{hull}/B_0) is chosen to satisfy the demand for using typical vessel dimensions as described in Section 3. Therefore, the beam (B_0) is adopted as a length-dependent parameter and is increased according to Eq. (7). The main vessel parameters for the variation of length are indicated in Table 2. Generally, a larger vessel is expected to show less roll amplitude than a smaller vessel in a similar sea state. Therefore, it can be expected that the larger vessel and therefore the more expensive vessel, will show an increase in operability. Exceptions to this general rule will be a focus of this investigation and can be found especially for the variation of beam (Section 4.5) and the variation of GM_T (Section 4.7).

4.5. Variation of beam

Favorable results in terms of percOP and ORI are found in the variation of beam as well for small vessel beams and shorter hull lengths in the North Sea for $L_{hull} = 80$ m and the North Atlantic for $L_{hull} \leq 100$ m, as well as for large vessel beams and larger hull lengths in the North Sea for $L_{hull} \geq 100$ m, and in the North Atlantic for $L_{hull} \geq 120$ m (Figs. 7 and 8). This means that, for example, during the North Atlantic winter season, the percOP for the 2° RMS roll criterion of an 80 m vessel with a beam of 15.3 m is around 80% and cannot be amplified by increasing the hull length unless the hull is at least 140 m long and has a beam of more than 29 m. This tendency is strongest during the winter season in the North Atlantic, and is less pronounced during the winter season in the North Sea and even more reduced during the summer season (Figs. 7 and 8).

Comparing the impact of the variation of beam in terms of deviation to its mean value of the individual length, the largest increase in percOP of 13.5% (absolute 84.6%) in North Sea and 26.0% (absolute 80.1%) in North Atlantic is found for the short vessel design with $L_{hull} = 80$ m and $B = 15.3$ m. The shortest vessel also shows the largest spread of percOP results within the same hull length of 18.7% for North Sea and 37.8% for North Atlantic for the 2° RMS roll limitation criterion. Whereas the results for the ORI are not showing a similar large spread in the results for the shortest hull length. Especially the influence of the beam

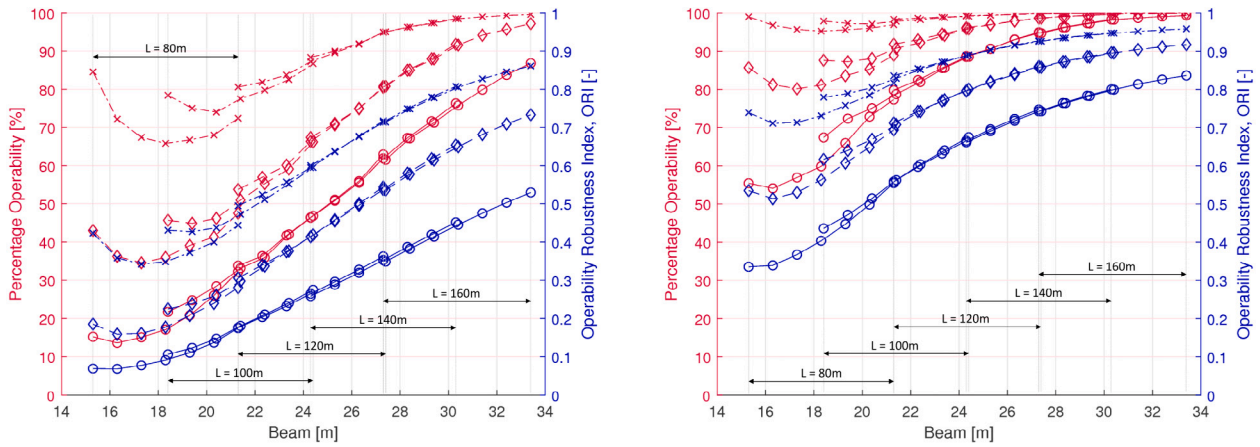


Fig. 7. North Sea. Beam variation in winter- (left) and summer season (right). For coloured representations consult the open access web version.

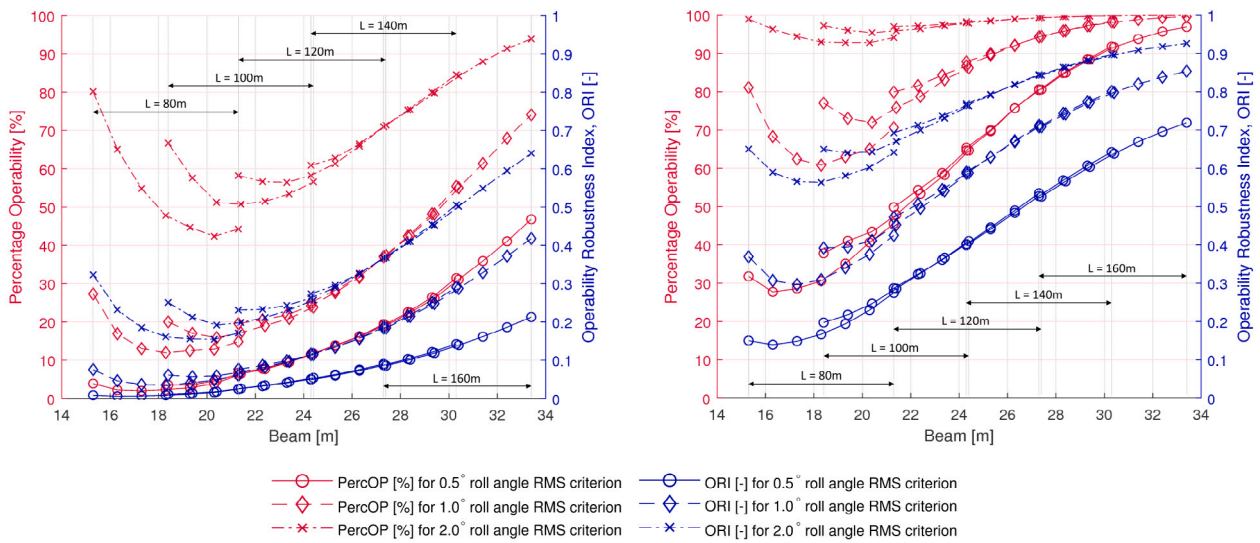


Fig. 8. North Atlantic. Beam variation in winter- (left) and summer season (right). For coloured representations consult the open access web version.

| | | Absolute value for beam variation | | | | | | | Deviation from mean for beam variation | | | | | | | | | |
|------------|----------------|-----------------------------------|-------|------|-------|-------|------|-------|--|--------|-------|-------|-------|-------|-------|-------|-------|-------|
| | | Length [m] | small | mid | large | small | mid | large | Mean | Spread | small | mid | large | small | mid | large | | |
| percOP [%] | North Sea | 80 | 84.6 | 72.2 | 67.4 | 65.8 | 66.7 | 68.0 | 72.4 | 71.0 | 18.7 | 13.5 | 1.2 | -3.6 | -5.2 | -4.3 | -3.0 | 1.4 |
| | | 100 | 78.4 | 75.0 | 74.0 | 77.5 | 79.8 | 82.5 | 86.7 | 79.2 | 12.7 | -0.7 | -4.1 | -5.1 | -1.6 | 0.6 | 3.4 | 7.6 |
| | | 120 | 80.6 | 81.9 | 83.7 | 87.3 | 89.6 | 91.8 | 95.0 | 87.1 | 14.4 | -6.5 | -5.2 | -3.4 | 0.1 | 2.5 | 4.7 | 7.8 |
| | | 140 | 88.4 | 90.0 | 92.0 | 94.9 | 96.3 | 97.4 | 98.5 | 93.9 | 10.1 | -5.5 | -3.9 | -2.0 | 1.0 | 2.3 | 3.5 | 4.6 |
| | | 160 | 95.1 | 96.3 | 97.4 | 98.5 | 99.0 | 99.4 | 99.6 | 97.9 | 4.6 | -2.8 | -1.6 | -0.5 | 0.6 | 1.1 | 1.5 | 1.7 |
| percOP [%] | North Atlantic | 80 | 80.1 | 65.1 | 54.8 | 47.8 | 44.7 | 42.4 | 44.3 | 54.2 | 37.8 | 26.0 | 10.9 | 0.7 | -6.4 | -9.4 | -11.8 | -9.9 |
| | | 100 | 66.7 | 57.6 | 51.2 | 50.8 | 51.5 | 53.4 | 56.6 | 55.4 | 15.9 | 11.3 | 2.2 | -4.2 | -4.6 | -3.9 | -2.0 | 1.2 |
| | | 120 | 58.2 | 56.6 | 56.4 | 58.3 | 61.3 | 65.9 | 71.0 | 61.1 | 14.6 | -2.9 | -4.5 | -4.7 | -2.8 | 0.2 | 4.8 | 9.9 |
| | | 140 | 60.9 | 62.8 | 66.5 | 71.0 | 75.3 | 80.0 | 84.6 | 71.6 | 23.7 | -10.7 | -8.8 | -5.1 | -0.6 | 3.8 | 8.4 | 13.0 |
| | | 160 | 71.4 | 75.4 | 79.8 | 84.2 | 88.0 | 91.4 | 93.9 | 83.4 | 22.5 | -12.0 | -8.0 | -3.7 | 0.8 | 4.5 | 8.0 | 10.5 |
| ORI [-] | North Sea | 80 | 0.42 | 0.36 | 0.34 | 0.35 | 0.37 | 0.40 | 0.44 | 0.38 | 0.10 | 0.04 | -0.03 | -0.04 | -0.01 | 0.02 | 0.06 | |
| | | 100 | 0.43 | 0.43 | 0.44 | 0.47 | 0.51 | 0.55 | 0.60 | 0.49 | 0.17 | -0.06 | -0.06 | -0.05 | -0.02 | 0.02 | 0.06 | 0.11 |
| | | 120 | 0.50 | 0.52 | 0.56 | 0.60 | 0.64 | 0.68 | 0.72 | 0.60 | 0.22 | -0.11 | -0.08 | -0.04 | -0.01 | 0.04 | 0.08 | 0.12 |
| | | 140 | 0.60 | 0.64 | 0.68 | 0.71 | 0.75 | 0.78 | 0.81 | 0.71 | 0.21 | -0.11 | -0.07 | -0.03 | 0.00 | 0.04 | 0.07 | 0.10 |
| | | 160 | 0.71 | 0.75 | 0.78 | 0.80 | 0.83 | 0.85 | 0.86 | 0.80 | 0.15 | -0.08 | -0.05 | -0.02 | 0.01 | 0.03 | 0.05 | 0.06 |
| ORI [-] | North Atlantic | 80 | 0.32 | 0.23 | 0.19 | 0.16 | 0.16 | 0.16 | 0.17 | 0.20 | 0.17 | 0.13 | 0.03 | -0.01 | -0.04 | -0.04 | -0.04 | -0.03 |
| | | 100 | 0.25 | 0.21 | 0.19 | 0.20 | 0.21 | 0.23 | 0.26 | 0.22 | 0.07 | 0.03 | -0.01 | -0.03 | -0.02 | -0.01 | 0.01 | 0.04 |
| | | 120 | 0.23 | 0.23 | 0.24 | 0.26 | 0.29 | 0.33 | 0.37 | 0.28 | 0.14 | -0.05 | -0.05 | -0.04 | -0.02 | 0.01 | 0.05 | 0.09 |
| | | 140 | 0.27 | 0.30 | 0.33 | 0.37 | 0.41 | 0.45 | 0.51 | 0.38 | 0.23 | -0.10 | -0.08 | -0.05 | -0.01 | 0.03 | 0.08 | 0.13 |
| | | 160 | 0.37 | 0.41 | 0.45 | 0.50 | 0.55 | 0.60 | 0.64 | 0.50 | 0.27 | -0.13 | -0.09 | -0.05 | 0.00 | 0.05 | 0.09 | 0.14 |

Fig. 9. Absolute and relative results for beam variation and 2° roll angle RMS criterion. For coloured representations consult the open access web version.

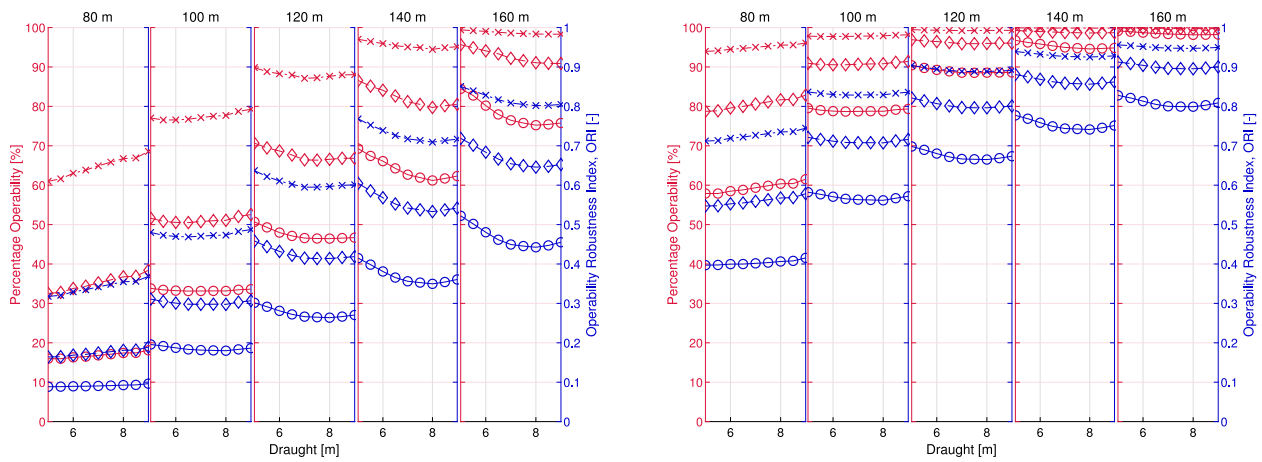


Fig. 10. North Sea. Draught variation during winter- (left) and summer season (right). For coloured representations consult the open access web version.

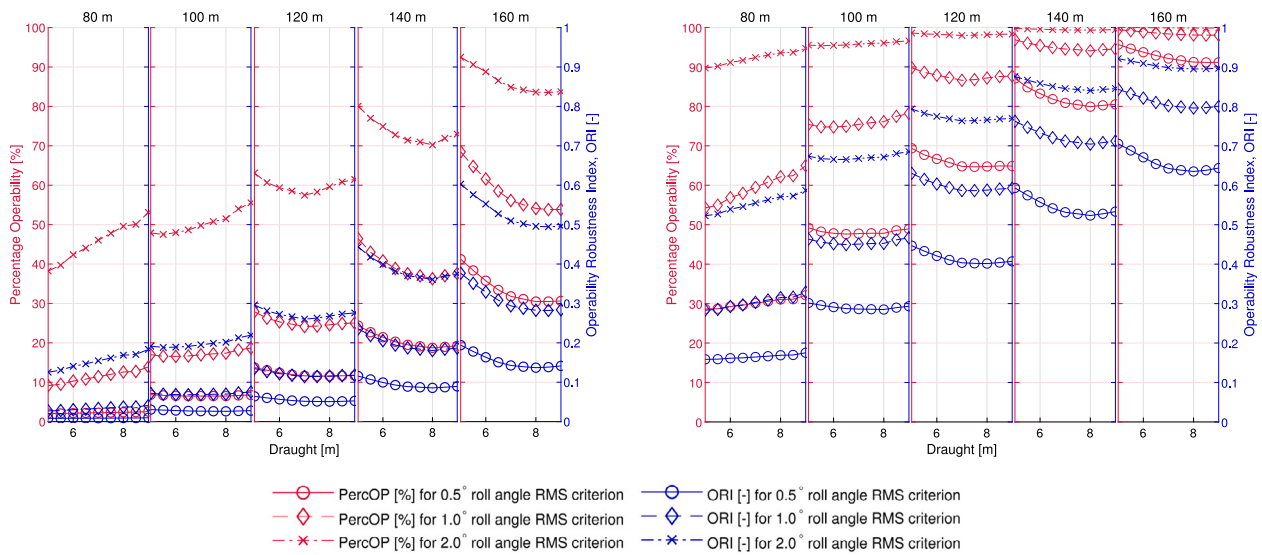


Fig. 11. North Atlantic. Draught variation during winter- (left) and summer season (right). For coloured representations consult the open access web version.

| | | Absolute value for draught variation | | | | | | | | | | Deviation from mean for draught variation | | | | | | | | | | |
|------------|----------------|--------------------------------------|-------|-------|-------|-------|-------|-------|-------|-------|-------|---|--------|-------|-------|-------|-------|-------|-------|-------|-------|-------|
| | | Length [m] | 5.0 m | 5.5 m | 6.0 m | 6.5 m | 7.0 m | 7.5 m | 8.0 m | 8.5 m | 9.0 m | Mean | Spread | 5.0 m | 5.5 m | 6.0 m | 6.5 m | 7.0 m | 7.5 m | 8.0 m | 8.5 m | 9.0 m |
| percOP [%] | North Sea | 80 | 61.0 | 61.6 | 63.0 | 63.8 | 64.9 | 65.8 | 66.7 | 66.9 | 68.6 | 64.7 | 7.57 | -3.7 | -3.1 | -1.7 | -0.9 | 0.2 | 1.1 | 2.0 | 2.2 | 3.8 |
| | | 100 | 77.1 | 76.5 | 76.6 | 76.7 | 77.2 | 77.5 | 77.7 | 78.7 | 79.3 | 77.5 | 2.72 | -0.4 | -0.9 | -0.7 | -0.3 | 0.0 | 0.2 | 1.2 | 1.8 | |
| | | 120 | 89.8 | 88.8 | 88.3 | 88.0 | 87.1 | 87.3 | 87.6 | 88.0 | 88.1 | 88.1 | 2.73 | 1.7 | 0.7 | 0.2 | -0.1 | -1.0 | -0.9 | -0.5 | -0.1 | -0.1 |
| | | 140 | 97.0 | 96.5 | 95.9 | 95.4 | 95.1 | 94.9 | 94.5 | 94.9 | 95.1 | 95.1 | 2.58 | 1.6 | 1.0 | 0.5 | -0.1 | -0.4 | -0.6 | -1.0 | -0.6 | -0.3 |
| | | 160 | 99.4 | 99.2 | 99.0 | 98.8 | 98.6 | 98.5 | 98.5 | 98.4 | 98.3 | 98.3 | 98.7 | 1.09 | 0.7 | 0.5 | 0.3 | 0.1 | -0.1 | -0.3 | -0.4 | -0.4 |
| percOP [%] | North Atlantic | 80 | 38.2 | 39.7 | 42.4 | 44.0 | 46.1 | 47.8 | 49.6 | 50.1 | 53.1 | 45.7 | 14.87 | -7.4 | -5.9 | -3.3 | -1.6 | 0.4 | 2.1 | 3.9 | 4.4 | 7.4 |
| | | 100 | 47.9 | 47.5 | 48.0 | 48.6 | 49.8 | 50.8 | 51.5 | 54.0 | 55.5 | 50.4 | 8.02 | -2.5 | -2.9 | -2.4 | -1.8 | -0.6 | 0.4 | 1.1 | 3.6 | 5.1 |
| | | 120 | 63.1 | 60.7 | 59.4 | 58.5 | 57.5 | 58.3 | 59.6 | 60.8 | 61.5 | 59.9 | 5.63 | 3.2 | 0.7 | -0.6 | -1.4 | -2.5 | -1.6 | -0.3 | 0.9 | 1.5 |
| | | 140 | 80.1 | 77.0 | 74.9 | 72.8 | 71.4 | 71.0 | 70.2 | 71.9 | 73.0 | 73.6 | 9.84 | 6.5 | 3.4 | 1.3 | -0.8 | -2.2 | -2.6 | -3.4 | -1.7 | -0.6 |
| | | 160 | 92.5 | 90.6 | 88.8 | 86.6 | 84.9 | 84.2 | 83.6 | 83.5 | 83.7 | 86.5 | 8.94 | 6.0 | 4.1 | 2.3 | 0.1 | -1.6 | -2.3 | -2.9 | -2.9 | -2.8 |
| ORI [-] | North Sea | 80 | 0.32 | 0.32 | 0.33 | 0.33 | 0.34 | 0.35 | 0.35 | 0.36 | 0.37 | 0.34 | 0.05 | -0.02 | -0.02 | -0.01 | -0.01 | 0.00 | 0.01 | 0.01 | 0.01 | 0.03 |
| | | 100 | 0.48 | 0.47 | 0.47 | 0.47 | 0.47 | 0.47 | 0.47 | 0.48 | 0.49 | 0.48 | 0.02 | 0.00 | 0.00 | -0.01 | -0.01 | 0.00 | 0.00 | 0.00 | 0.01 | 0.01 |
| | | 120 | 0.64 | 0.62 | 0.61 | 0.60 | 0.59 | 0.60 | 0.60 | 0.60 | 0.60 | 0.61 | 0.04 | 0.03 | 0.02 | 0.00 | 0.00 | -0.01 | -0.01 | -0.01 | -0.01 | -0.01 |
| | | 140 | 0.77 | 0.75 | 0.74 | 0.73 | 0.72 | 0.71 | 0.71 | 0.71 | 0.72 | 0.73 | 0.06 | 0.04 | 0.02 | 0.01 | 0.00 | -0.01 | -0.01 | -0.02 | -0.02 | -0.01 |
| | | 160 | 0.85 | 0.84 | 0.83 | 0.82 | 0.81 | 0.80 | 0.80 | 0.80 | 0.80 | 0.82 | 0.05 | 0.03 | 0.02 | 0.01 | 0.00 | -0.01 | -0.01 | -0.02 | -0.02 | -0.01 |
| ORI [-] | North Atlantic | 80 | 0.13 | 0.13 | 0.14 | 0.15 | 0.15 | 0.16 | 0.17 | 0.17 | 0.18 | 0.15 | 0.06 | -0.03 | -0.02 | -0.01 | -0.01 | 0.00 | 0.01 | 0.02 | 0.02 | 0.03 |
| | | 100 | 0.19 | 0.19 | 0.19 | 0.19 | 0.20 | 0.20 | 0.20 | 0.21 | 0.22 | 0.20 | 0.03 | -0.01 | -0.01 | -0.01 | -0.01 | 0.00 | 0.00 | 0.00 | 0.01 | 0.02 |
| | | 120 | 0.30 | 0.28 | 0.27 | 0.27 | 0.26 | 0.26 | 0.27 | 0.27 | 0.28 | 0.27 | 0.04 | 0.02 | 0.01 | 0.00 | -0.01 | -0.01 | -0.01 | 0.00 | 0.00 | 0.00 |
| | | 140 | 0.44 | 0.42 | 0.40 | 0.38 | 0.37 | 0.37 | 0.36 | 0.37 | 0.38 | 0.39 | 0.08 | 0.06 | 0.03 | 0.01 | -0.01 | -0.02 | -0.02 | -0.03 | -0.02 | -0.01 |
| | | 160 | 0.60 | 0.58 | 0.55 | 0.53 | 0.51 | 0.50 | 0.50 | 0.49 | 0.50 | 0.53 | 0.11 | 0.07 | 0.05 | 0.02 | 0.00 | -0.02 | -0.03 | -0.03 | -0.03 | -0.03 |

Fig. 12. Absolute and relative results for draught variation and 2° roll angle RMS criterion. For coloured representations consult the open access web version.

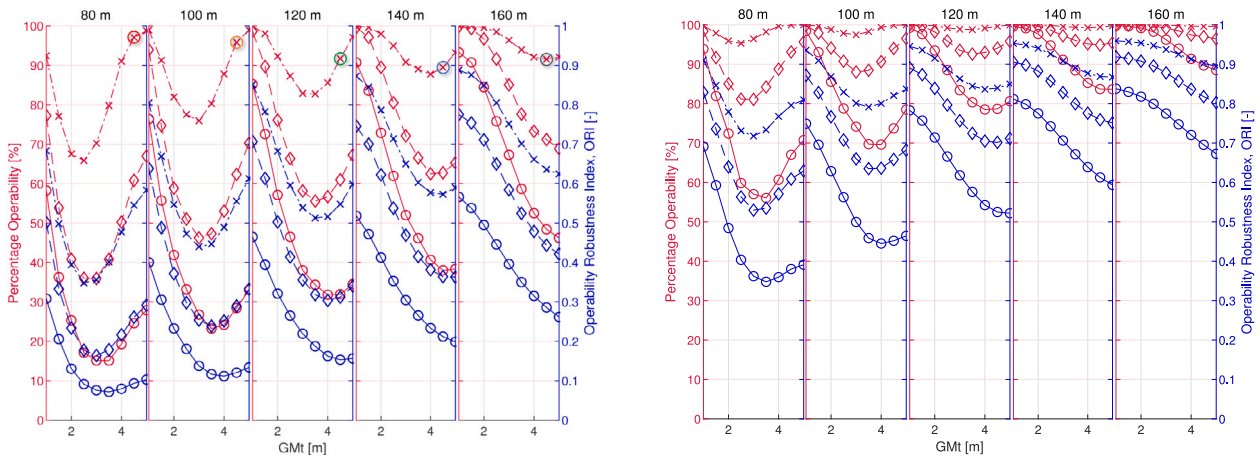


Fig. 13. North Sea. GM_t variation during winter- (left) and summer season (right). For coloured representations consult the open access web version.

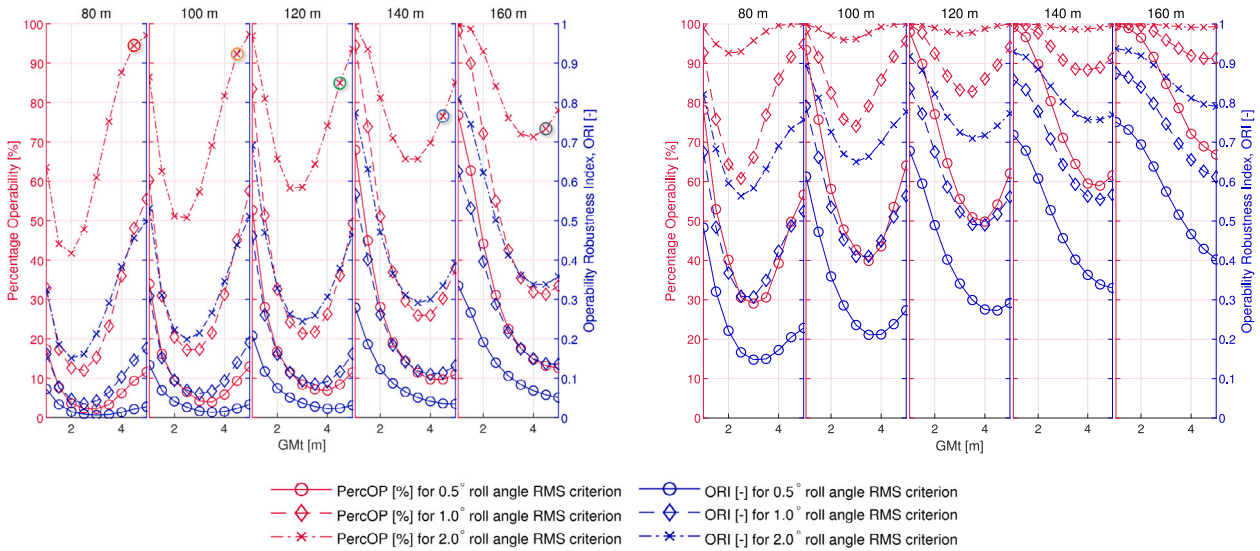


Fig. 14. North Atlantic. GM_t variation during winter- (left) and summer season (right). For coloured representations consult the open access web version.

| | | Absolute value for metacentric height variation | | | | | | | | | Deviation from mean for metacentric height variation | | | | | | | | | | | |
|----------------|----------------|---|-------|-------|-------|-------|-------|-------|-------|-------|--|--------|-------|-------|-------|-------|-------|-------|-------|-------|-------|-------|
| | | 1.0 m | 1.5 m | 2.0 m | 2.5 m | 3.0 m | 3.5 m | 4.0 m | 4.5 m | 5.0 m | Mean | Spread | 1.0 m | 1.5 m | 2.0 m | 2.5 m | 3.0 m | 3.5 m | 4.0 m | 4.5 m | 5.0 m | |
| percOP [%] | North Sea | 80 | 92.4 | 77.0 | 67.5 | 65.8 | 70.2 | 79.8 | 91.0 | 97.0 | 98.7 | 82.2 | 32.9 | 10.2 | -5.1 | -14.7 | -16.3 | -12.0 | -2.4 | 8.8 | 14.9 | 16.5 |
| | | 100 | 98.9 | 91.2 | 81.9 | 77.5 | 75.9 | 80.3 | 87.8 | 95.8 | 98.9 | 87.6 | 23.0 | 11.3 | 3.7 | -5.6 | -10.1 | -11.7 | -7.3 | 0.2 | 8.2 | 11.3 |
| | | 120 | 99.9 | 98.0 | 92.3 | 87.3 | 82.9 | 82.7 | 85.6 | 91.7 | 97.1 | 90.8 | 17.1 | 9.1 | 7.2 | 1.4 | -3.6 | -7.9 | -8.1 | -5.3 | 0.9 | 6.3 |
| | | 140 | 100.0 | 99.6 | 97.9 | 94.9 | 90.8 | 89.0 | 87.7 | 89.5 | 93.2 | 93.6 | 12.3 | 6.4 | 6.0 | 4.3 | 1.3 | -2.8 | -4.6 | -5.9 | -4.2 | -0.5 |
| | | 160 | 100.0 | 100.0 | 99.6 | 98.5 | 96.3 | 93.9 | 92.1 | 91.5 | 92.1 | 96.0 | 8.5 | 4.0 | 4.0 | 3.6 | 2.5 | 0.4 | -2.1 | -3.9 | -4.5 | -3.9 |
| ORI [-] | North Atlantic | 80 | 63.5 | 44.1 | 41.7 | 47.8 | 61.0 | 75.2 | 87.6 | 94.4 | 97.1 | 68.1 | 55.3 | -4.5 | -23.9 | -26.3 | -20.3 | -7.0 | 7.1 | 19.6 | 26.4 | 29.0 |
| | | 100 | 86.5 | 62.5 | 51.2 | 50.8 | 57.3 | 69.1 | 81.7 | 92.3 | 97.3 | 72.1 | 46.6 | 14.4 | -9.5 | -20.9 | -21.3 | -14.7 | -3.0 | 9.6 | 20.2 | 25.2 |
| | | 120 | 96.9 | 81.0 | 65.7 | 58.3 | 58.5 | 64.4 | 74.1 | 85.0 | 93.6 | 75.3 | 38.7 | 21.7 | 5.7 | -9.6 | -17.0 | -16.8 | -10.9 | -1.2 | 9.7 | 18.4 |
| | | 140 | 99.4 | 93.5 | 81.2 | 71.0 | 65.7 | 65.7 | 69.7 | 76.6 | 85.2 | 78.7 | 33.7 | 20.8 | 14.8 | 2.6 | -7.7 | -13.0 | -13.0 | -8.9 | -2.1 | 6.5 |
| | | 160 | 100.0 | 98.7 | 93.0 | 84.2 | 76.1 | 72.0 | 71.3 | 73.3 | 78.0 | 82.9 | 28.7 | 17.0 | 15.8 | 10.0 | 1.2 | -6.9 | -11.0 | -11.7 | -9.6 | -4.9 |
| North Sea | 80 | 0.68 | 0.50 | 0.39 | 0.35 | 0.36 | 0.40 | 0.48 | 0.54 | 0.58 | 0.48 | 0.33 | 0.21 | 0.02 | -0.08 | -0.13 | -0.12 | -0.08 | 0.00 | 0.07 | 0.11 | |
| | | 100 | 0.80 | 0.67 | 0.55 | 0.47 | 0.44 | 0.45 | 0.49 | 0.56 | 0.61 | 0.36 | 0.36 | 0.25 | 0.11 | -0.01 | -0.09 | -0.12 | -0.11 | -0.07 | 0.00 | 0.05 |
| | | 120 | 0.85 | 0.78 | 0.68 | 0.60 | 0.54 | 0.51 | 0.52 | 0.55 | 0.60 | 0.62 | 0.34 | 0.23 | 0.16 | 0.06 | -0.03 | -0.09 | -0.11 | -0.11 | -0.08 | -0.03 |
| | | 140 | 0.87 | 0.84 | 0.79 | 0.71 | 0.65 | 0.60 | 0.58 | 0.57 | 0.59 | 0.69 | 0.30 | 0.18 | 0.15 | 0.10 | 0.02 | -0.04 | -0.09 | -0.11 | -0.12 | -0.10 |
| | | 160 | 0.89 | 0.88 | 0.85 | 0.80 | 0.75 | 0.70 | 0.66 | 0.64 | 0.62 | 0.75 | 0.26 | 0.13 | 0.12 | 0.09 | 0.05 | 0.00 | -0.05 | -0.09 | -0.12 | -0.13 |
| North Atlantic | 80 | 0.32 | 0.19 | 0.15 | 0.16 | 0.21 | 0.29 | 0.38 | 0.46 | 0.50 | 0.30 | 0.35 | 0.03 | -0.11 | -0.14 | -0.13 | -0.08 | 0.00 | 0.09 | 0.16 | 0.20 | |
| | | 100 | 0.53 | 0.31 | 0.22 | 0.20 | 0.21 | 0.27 | 0.35 | 0.44 | 0.51 | 0.34 | 0.33 | 0.19 | -0.03 | -0.12 | -0.14 | -0.12 | -0.07 | 0.01 | 0.10 | 0.17 |
| | | 120 | 0.69 | 0.47 | 0.33 | 0.26 | 0.24 | 0.26 | 0.31 | 0.38 | 0.46 | 0.38 | 0.45 | 0.31 | 0.09 | -0.05 | -0.12 | -0.13 | -0.12 | -0.07 | 0.00 | 0.09 |
| | | 140 | 0.77 | 0.63 | 0.47 | 0.37 | 0.31 | 0.29 | 0.30 | 0.33 | 0.39 | 0.43 | 0.48 | 0.34 | 0.20 | 0.04 | -0.06 | -0.12 | -0.14 | -0.13 | -0.10 | -0.04 |
| | | 160 | 0.81 | 0.74 | 0.62 | 0.50 | 0.41 | 0.36 | 0.34 | 0.34 | 0.36 | 0.50 | 0.47 | 0.31 | 0.25 | 0.12 | 0.00 | -0.09 | -0.14 | -0.16 | -0.16 | -0.14 |

Fig. 15. Absolute and relative results for GM_t variation and 2° roll angle RMS criterion. For coloured representations consult the open access web version.

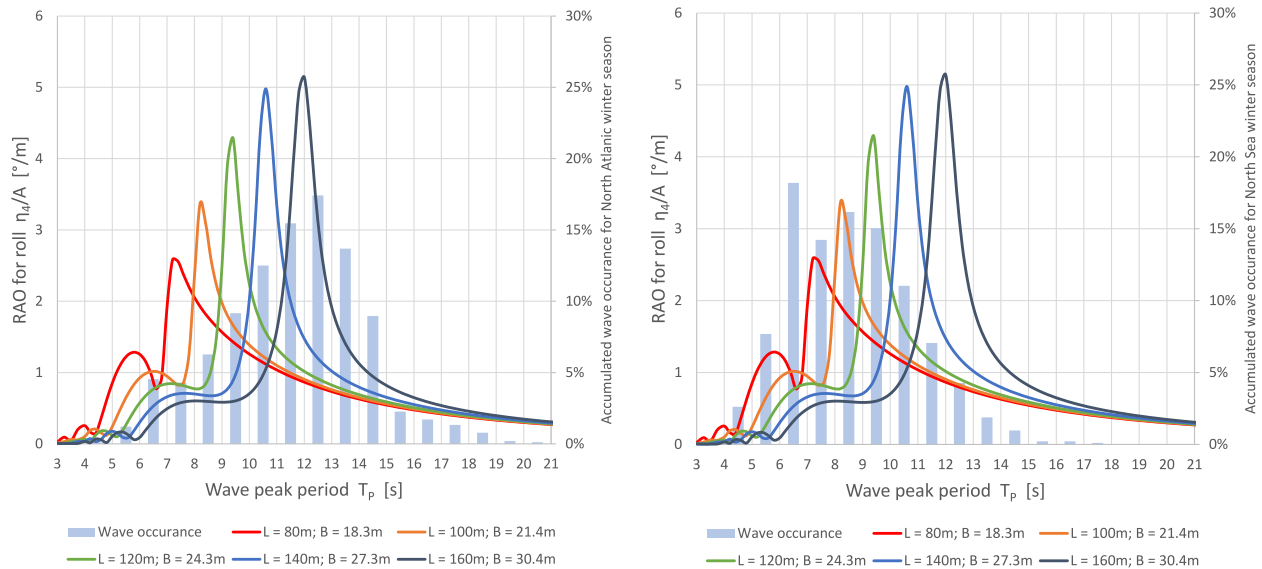


Fig. 16. Roll motion RAO in relation to the wave occurrence accumulated over the wave height per peak period. For coloured representations consult the open access web version.

variation in the North Sea shows less spread for shorter hull length, indicating that the results for a more restrictive limitation criterion might be better for wider hulls given that GM_T can be kept small. In the North Sea the ORI value shows that for the 80 m vessel an especially narrow and wide vessel will be favorable, while in the North Atlantic the narrow hull of this hull length performs clearly better than the wide hull. This behavior is opposite for $L_{hull} \geq 100$ m in the North Sea and $L_{hull} \geq 120$ m in the North Atlantic.

From the results for the variation of beam, it can be seen that the information value of percOP as performance indicator highly depends on the choice of the level for the maximal acceptable limitation criterion. This can be acceptable if a vessel will be selected for a certain operational task, however, for design purposes, the ORI provides a more general limitation criterion, less dependent on the limitation criterion level. Nevertheless, the results of both benchmarking criteria, especially for intermediate hull lengths, are dependent on the choice of the specific sea area providing a certain wave energy spectrum for individual peak periods.

Commonly, the results of the beam variation show that typical length to beam ratios for offshore vessels, as used for the mid-range settings shown in Table 2, show rather unfavorable seakeeping performance.

4.6. Variation of draught

The variation of draught is performed for all ship lengths, corresponding a draught range between 5 m and 9 m in 0.5 m steps. Generally, the variation of draught shows minor impact on percOP and ORI. A slightly beneficial performance is found for large draughts at shorter hull length ($L_{hull} \leq 100$ m) and thus smaller beam values ($B_0 \leq 21.30$ m) as well as for low draught for longer hull length ($L_{hull} \geq 120$ m) and thus larger beam values ($B_0 \geq 24.30$ m; Figs. 10 and 11). The largest spread in terms of percOP of about 14.9% can be found in the results for the North Atlantic for the 80 m long vessel design (Fig. 12). The impact of draught variation on roll performance is rather small for the medium-sized hull designs of 100 m and 120 m hull length. The results for the ORI are in accordance with the results for the percOP.

In contrast to the variation of beam and GM_T , the draught variation has no influence on the vessel's natural roll period and thus shows similar results for both sea areas. The variation of draught will rather influence roll damping due to minor viscous and more considerable added mass effects. Especially the larger roll reduction for smaller

draught and longer-, and wider vessel designs can be explained by increased added mass effects. Similar to a catamaran, a flat and wide cross sectional shape may induce more vertical than rotatory motions at the outside hull area. Therefore, the heave-like motion component may increase roll damping due to added mass effects for low draught at larger beams. It may be noted that for the variation of draught the vertical center of gravity (VCG) is adjusted to keep a constant GM_T as indicated in Table 4.

4.7. Variation of metacentric height

The variation of metacentric height (GM_T) is performed for all ship lengths for GM_T values between 1 m and 5 m in 0.5 m steps. The GM_T level is strongly affecting the vessel's roll period and shows thus a strong influence on roll performance in terms of percOP and ORI in the analyzed sea areas (Figs. 13 and 14). To obtain small roll angles, generally, a small GM_T value, resulting in a longer roll period (with *soft* motion characteristics), as well as a large GM_T value, resulting in a shorter roll period (with *stiff* motion characteristics) is favorable. The unfavorable region of low performance GM_T is shifting from smaller GM_T values (of around 2.0 m) for shorter vessel designs (80 m) to larger GM_T values (of around 4.0 m) for longer vessel designs (160 m, Fig. 15).

The results of percOP for the vessel design with $GM_T = 4.5$ m are marked in Figs. 13 and 14 by color-coded circles referring to the similar colored RAOs shown in Fig. 16. Especially, the results analyzed for the North Atlantic winter season indicate for the shortest hull length ($L_{hull} = 80$ m) a significantly better roll performance than for the larger vessel ($L_{hull} = 160$ m) with the same GM_T value. The corresponding absolute percOP values can be found additionally in Fig. 15 (see column showing results for $GM_T = 4.5$ m). An explanation for this atypical result is indicated in Fig. 16 showing the RAOs for the five corresponding vessel designs in relation to the wave occurrences, shown as accumulation of H_S per T_p , over the wave peak period T_p . This presentation indicates that the sensitive period of the maximal response amplitude of the small designs is clearly distinct from the dominating wave periods observed during the North Atlantic winter season, while this is not the case for the analysis performed for the North Sea winter season. Hence, the roll response amplitude of the smaller vessel is favorable above the large vessel operating during the North Atlantic winter season.

It has to be noted that there are existing stability requirements limiting small GM_T values, not allowing it to fall below a value in an order

of around 1.0 m. Considering $GM_T \geq 1.5$ m, it can be concluded that shorter vessels ($L_{hull} \leq 120$ m) show a higher operational performance for larger GM_T values ($GM_T \geq 4.5$ m) and large vessels ($L_{hull} \geq 140$ m) show a higher operational performance for smaller GM_T values. The influence on maximal tolerable accelerations of a softer versus a stiffer vessel must be further evaluated.

5. Summary

The selection and optimization of a vessel design to perform a specific offshore operational task, considering costs and operational aspects, is not straightforward and requires detailed comparative operability analyses. However, according to information provided by offshore vessel designer's, today's common practice is to perform seakeeping analysis for the approval of a final design only. Although it might be expected that roll amplitudes of a larger vessel will be smaller and hence more favorable than those of a smaller vessel, this study shows that this assumption is not always true. A key aspect of a design process should be the mission-dependent optimization of hull dimensions, including loading condition parameters, aiming for a design where natural periods of important responses such as pitch and roll are significantly different from the dominating wave periods. This research focuses on the quantification of the relative impact of design variations on seakeeping performance at zero speed aiming for the identification of weather-robust vessel designs, as a requirement to operate safely in higher sea states.

For the identification and benchmarking of mission-oriented vessel capabilities this research utilizes two seakeeping performance parameters, the percentage operability (percOP) and the newly developed Operational Robustness Index (ORI). The paper presents that a well established percOP performance indicator is a suitable parameter for operational planning and vessel selection, if all operational details are available, while the ORI clearly indicates advantages for design optimization during the early ship design process, and for vessel selection, in circumstances when operational limitations, sea area, or season are not specified. As a consequence, the ORI can be judged as the more robust performance criterion since it is less sensitive to user input. In this analysis the advantages of the ORI are described in cases when seakeeping performance is generally good and when the percOP value converges against 100%, and hence does not indicate a generally better performing vessel, while the ORI remains capable of indicating differences in performance.

Results of a parametric study of design characteristics indicate a significant influence on roll performance for the variation of hull length, beam and metacentric height (GM_T), whereas minor deviations for the variation of draught are found. As a general result, it can be concluded that seakeeping performance is often increasing with vessel dimensions. However, this rule does not necessarily apply to the selection of beam and GM_T parameters. As an example from the results of the beam variation during North Atlantic winter season, favorable seakeeping performance is found for small vessel beams and shorter hull length as well as for large vessel beams and larger hull length. To further illustrate this, the roll performance of an 80 m vessel with a beam of 15.3 m is around 80% and cannot be improved by increasing hull length unless the hull is at least 140 m long and has a beam of more than 29 m.

Similar to the choice of the hull beam, the choice of the vertical center of gravity and hence GM_T is strongly influencing the vessel's roll performance. Favorable results are found for both small and large GM_T values, whereas for OCVs often adopted GM_T values of 2 m to 3 m show an unfavorable roll performance and thus larger roll angles. The advantage of a larger GM_T value is more pronounced for shorter hull length which is resulting in the fact that the shortest hull length of 80 m with a GM_T parameter of 4.5 m performs significantly better than the largest vessel of 160 m length with the same GM_T value. As an explanation of this phenomenon it is indicated that in such cases the peak period for the maximum amplitude of the Response Amplitude

Operator (RAO) for roll clearly differs from the peak period of the dominating wave energy.

Due to the large amount of data generated in this research project, the presented study is limited to the analysis of the impact of hull length, beam, draught, and GM_T variation on seakeeping performance, utilizing the roll amplitude criterion at zero speed and 30° wave heading. Therefore, the interested reader is invited to perform further analysis using the Vessel Response Tool, for free online available on vrt.sintef.no.

6. Conclusion

The study has shown that vessel size is not always the decisive parameter for the determination of seakeeping performance. Therefore, the simple rule *bigger is better* does not apply in all cases. The findings on the variation of beam and GM_T show that commonly adopted values are rather unfavorable regarding roll performance. Therefore, a significant potential for the minimization of the vessel's roll amplitude and thus the improvement of seakeeping performance is given. This potential must be used for design optimization and will contribute to increased operability towards year-round offshore operations as well as to cost reductions of offshore installation and maintenance services. As benchmarking parameter, this investigation utilizes a novel seakeeping performance indicator, the Operability Robustness Index (ORI) and compares its application with the widely known percentage operability value. The comparison of these two performance indicators clearly indicate the advantage of using the ORI for seakeeping optimization. The ORI can be judged as the more robust performance indicator identifying improvements in seakeeping performance for a selected sea area more correctly independently of the magnitude of the limitation criterion. Additional to the results presented, the reader is invited to further explore the ORI as seakeeping performance criterion for offshore vessels using the Vessel Response Tool, accessible for free on vrt.sintef.no.

CRedit authorship contribution statement

Martin Gutsch: Conceptualization, Methodology, Formal analysis, Investigation, Writing - original draft, Writing - review & editing, Visualization. **Sverre Steen:** Supervision, Writing - review & editing. **Florian Sprenger:** Supervision, Writing - review & editing.

Declaration of competing interest

The authors declare that they have no known competing financial interests or personal relationships that could have appeared to influence the work reported in this paper.

Acknowledgment

This work was made possible through the Centre of Research-based Innovation SFI MOVE, financially supported by the Norwegian Research Council, NFR project number 237929 and the consortium partners, <http://www.ntnu.edu/move>.

References

- Bales, N.K., Cummins, W.E., 1970. The influence of hull form on seakeeping. In: Cummins, W.E., The Society of Naval, A., Marine, E. (Eds.), *Annual Meeting SNAME*. SNAME, New York.
- Bengtsson, B.G., 1962. Influence of V and U Shaped Fore Body Sections of Motions and Propulsion of Ships in Waves. Report Nr. 49, In: *Meddelanden (Statens skeppsprovninganstalt)*, Swedish State Shipbuilding Experimental Tank, Göteborg, Sweden.
- Bengtsson, B.B., 1965. Influence of V and U Shaped Fore Body Sections on Motions and Propulsion of Ships in Waves At Ballast Draught. In: *Meddelanden (Statens skeppsprovninganstalt)*, vol. 56, Swedish State Shipbuilding Experimental Tank, Göteborg.

- Beukelman, W., Huijser, A., 1976. Variation of Parameters Determining Seakeeping. Technical Report 443, Laboratorium voor Scheepshydronechanica.
- Comstock, E.N., Keane, R.G., 1980. Seakeeping by design. *Naval Engineers Journal* vol. 92, 157–178. <http://dx.doi.org/10.1111/j.1559-3584.1980.tb05267.x>.
- DNV GL, 2011. Marine Operations, General. Offshore Standard DNV-OS-H101.
- DNV GL, 2017. Environmental Conditions and Environmental Loads. Recommend Practice DNV-RP-C205.
- Ewing, J.A., 1967. The effect of speed, forebody shape and weight distribution on ship motions. *Transactions of the Royal Institution of Naval Architects* vol. 109, 337–346.
- Faltinsen, O.M., 1990. Sea Loads on Ships and Offshore Structures. In: Cambridge Ocean Technology Series, Cambridge University Press, Cambridge.
- Fathi, D., 2017. VERES User Manual. Report, SINTEF Ocean.
- Gutsch, M., Sprenger, F., Steen, S., 2016. Influence of design parameters on operability of offshore construction vessels. In: *Jahrbuch der Schiffbautechnischen Gesellschaft*. Schiffahrts-Verlag Hansa GmbH & Co. KG, Hamburg, pp. 230–242.
- Gutsch, M., Sprenger, F., Steen, S., 2017. Design parameters for increased operability of offshore crane vessels. In: ASME 2017 36th International Conference on Ocean, Offshore and Arctic Engineering. American Society of Mechanical Engineers (ASME).
- Himeno, Y., 1981. Prediction of Ship Roll Damping-State of the Art. Technical Report, University of Michigan.
- Ikeda, Y., Himeno, Y., Tanaka, N., 1976. On roll damping force of ship: Effects of friction of hull and normal force of bilge keels. *Journal of Society of Naval Architects of Japan* vol. 161, 41–49.
- Ikeda, Y., Himeno, Y., Tanaka, N., 1977a. On eddy making component of roll damping force on naked hull. *Journal of Society of Naval Architects of Japan* vol. 142, 54–64.
- Ikeda, Y., Komatsu, K., Himeno, Y., Tanaka, N., 1977b. On roll damping force of ship-effect of hull surface pressure created by bilge keels. *Journal of Society of Naval Architects of Japan* vol. 165, 31–40.
- Kato, H., 1957. On the frictional resistance to the rolling of ships. *Journal of Zosen Kiokai* vol. 102, 115–122.
- Lewis, E.V., 1955. Ship Speeds in Irregular Seas. Stevens Institute of Technology, Experimental Towing Tank, Hoboken, New Jersey, USA, Published by: The Society of Naval Architects and Marine Engineers, SNAME Transactions 1955, Paper No. 1, Paper: T1955-1 Transactions.
- Lloyd, A.R.J.M., 1989. Seakeeping: Ship Behaviour in Rough Weather. In: Ellis Horwood Series in Marine Technology, Ellis Horwood, Chichester.
- Loukakis, T.A., 1975. Seakeeping Standard Series for Cruiser-Stern Ships 3. SNAME, New York, p. 15.
- Lyng, I., Andreassen, D., Fiksdal, G.A.H., 2008. Official Norwegian reports: The loss of the “Bourbon Dolphin” on 12 April 2007. Departementenes Servicesenter, Informasjonsforvaltning, NOU, URL <https://towmasters.files.wordpress.com/2009/03/loss-of-the-bourbon-dolphin.pdf>.
- Mellbye, C.S., Jakobsen, E.W., Baustad, H., 2017. GCE Blue Maritime 2017 – Global Performance Benchmark. Report, Menon Economics.
- Papanikolaou, A., 2014. Ship Design: Methodologies of Preliminary Design. Springer.
- Salvesen, N., Tuck, E., Faltinsen, O., 1970. Ship motions and sea loads. *Trans. SNAME* 78, 250–287.
- Sandvik, E., Gutsch, M., Asbjørnslett, B.E., 2018. A simulation-based ship design methodology for evaluating susceptibility to weather-induced delays during marine operations. *Ship Technology Research* vol. 65, 137–152. <http://dx.doi.org/10.1080/09377255.2018.1473236>.
- Swaan, W., 1961. The influence of principal dimensions on ship behaviour in irregular waves. *International Shipbuilding Progress* vol. 8, 248–254.
- Swaan, W., Vossers, G., 1961. The effect of forebody section shape on ship behaviour in waves. *International Shipbuilding Progress* vol. 8, 279–301.
- Young, I.R., Ribal, A., 2019. Multiplatform evaluation of global trends in wind speed and wave height. *Science* <http://dx.doi.org/10.1126/science.aav9527>.
- Yourkov, N., 1973. Vertical motions of ships with different form of forebody. *International Shipbuilding Progress* vol. 20, 57–71.